Title: Local adaptation to climate facilitates a global invasion

Authors: Diana Gamba[1]*, Megan L. Vahsen[2], Toby M. Maxwell[3], Nikki Pirtel[2], Seth Romero[4], Justin J. Van Ee[5], Amanda Penn[1], Aayudh Das[1], Rotem Ben-Zeev[1], Owen Baughman[6], C. Sean Blaney[7], Randy Bodkins[8], Shanta Budha-Magar[9], Stella M. Copeland[10], Shannon L. Davis-Foust[11], Alvin Diamond[12], Ryan C. Donnelly[13], Peter W. Dunwiddie[14], David J. Ensing[15], Thomas A. Everest[16], Holly Hoitink[8], Martin C. Holdrege[17], Ruth A. Hufbauer[5], Sigitas Juzėnas[18], Jesse M. Kalwij[19], Ekaterina Kashirina[20], Sangtae Kim[21], Marcin Klisz[22], Alina Klyueva[23], Michel Langeveld[8], Samuel Lutfy[24], Daniel Martin[8], Christopher L. Merkord[25], John W. Morgan[26], Dávid U. Nagy[27], Jacqueline P. Ott[28], Radoslaw Puchalka[29], Lysandra A. Pyle[30], Leonid Rasran[31], Brian G. Rector[32], Christoph Rosche[27], Marina Sadykova[8], Robert K. Shriver[33], Alexandr Stanislavschi[34], Brian M. Starzomski[35], Rachel L. Stone[36], Kathryn G. Turner[37], Alexandra K. Urza[38], Acer VanWallendael[39], Carl-Adam Wegenschimmel[40], Justin Zweck[41], Cynthia S. Brown[5], Elizabeth A. Leger[42], Dana M. Blumenthal[4], Matthew J. Germino[43], Lauren M. Porensky[4], Mevin B. Hooten[44], Peter B. Adler[2], Jesse R. Lasky[1]

Affiliations:

[1] Department of Biology, Pennsylvania State University; University Park, PA, USA.
*Corresponding author. Email: dxg5484@psu.edu

[2] Department of Wildland Resources and the Ecology Center, Utah State University; Logan, UT, USA.

[3] Department of Biological Sciences, Boise State University; Boise, ID, USA.

[4] US Department of Agriculture, Agricultural Research Service, Rangeland Resources and Systems Research Unit; Fort Collins, CO, USA.

[5] Department of Agricultural Biology, Colorado State University; Fort Collins, CO, USA.

[6] The Nature Conservancy; Burns, OR, USA.

[7] Atlantic Canada Conservation Data Centre; Sackville, NB, Canada.

[8] Not affiliated.

[9] Northtec; Whangarei, New Zealand.

[10] US Department of Agriculture, Agricultural Research Service, Eastern Oregon Agricultural Research Center; Burns, OR, USA.

[11] Biology Department, University of Wisconsin Oshkosh; Oshkosh, WI, USA.

[12] Department of Biological and Environmental Sciences, Troy University; Troy, Alabama, USA.

[13] Division of Biology, Kansas State University; Manhattan, KS, USA.

[14] Department of Biology, University of Washington; Seattle, WA, USA.

[15] Summerland Research and Development Centre, Agriculture and Agri-Food Canada; Summerland, BC, Canada.

[16] Department of Entomology, Cornell University; Ithaca, NY, USA.

[17] Northern Arizona University, Center for Adaptable Western Landscapes; Flagstaff, AZ, USA.

[18] Department of Botany and Genetics, Institute of Biosciences, Life Sciences Center, Vilnius University; Vilnius, Lithuania.

[19] Institute of Geography and Geoecology, Karlsruhe Institute of Technology; Karlsruhe, Germany.

[20] Moscow State University; Moscow, Russia.

[21] Department of Biology, Sungshin Women's University; Seoul, Republic of Korea.

[22] Department of Silviculture and Genetics of Forest Trees, Forest Research Institute; Raszyn, Poland.

[23] Bryansk State University named after Academician I. G. Petrovsky; Bryansk, Russia.

[24] Caesar Kleberg Wildlife Research Institute, Texas A&M University - Kingsville; Kingsville, TX, USA.

[25] Biosciences Department, Minnesota State University Moorhead; Moorhead, MN, USA.

[26] Department of Environment and Genetics, La Trobe University; Bundoora, Victoria, Australia.

[27] Institute of Biology/Geobotany and Botanical Garden, Martin Luther University Halle-Wittenberg; Halle, Saale, Germany.

[28] USDA Forest Service, Rocky Mountain Research Station, Rapid City, SD, USA.

[29] Department of Ecology and Biogeography, Nicolaus Copernicus University; Torun, Poland.

[30] Alberta Biodiversity Monitoring Institute; Edmonton, AB, Canada.

[31] University of Natural Resources and Life Sciences, Vienna; Vienna, Austria.

[32] US Department of Agriculture, Agricultural Research Service, Invasive Species and Pollinator Health Research Unit; Albany, CA, USA.

[33] Department of Natural Resources and Environmental Science, University of Nevada; Reno, NV, USA.

[34] Department of Organic, Biochemical, and Food Engineering, Gheorghe Asachi Technical University of Iasi; Iasi, Romania.

[35] School of Environmental Studies, University of Victoria; Victoria, BC, Canada.

[36] Department of Biology, Case Western Reserve University; Cleveland, OH, USA.

[37] Department of Biological Sciences, Idaho State University; Pocatello, ID, USA.

[38] USDA Forest Service, Rocky Mountain Research Station, Reno, NV, USA.

[39] Department of Horticultural Science, North Carolina State University; Raleigh, NC, USA.

[40] Terrastory Environmental Consulting Inc.; Hamilton, ON, Canada.

[41] Department of Ecosystem Science and Management, Pennsylvania State University; University Park, PA, USA.

[42] Department of Biology, University of Nevada; Reno, NV, USA.

[43] US Geological Survey, Forest and Rangeland Ecosystem Science Center; Boise, Idaho, USA.

[44] Department of Statistics and Data Sciences, The University of Texas at Austin; Austin, TX, USA.

Abstract: Local adaptation may facilitate range expansion during invasions, but the mechanisms promoting destructive invasions remain unclear. Cheatgrass (*Bromus tectorum*), native to Eurasia and Africa, has invaded globally, with particularly severe impacts in western North America. We sequenced 307 genotypes and conducted controlled experiments. We found that diverse lineages invaded North America, where long-distance gene flow is common. Ancestry and phenotypic clines in the native range predicted those in the invaded range, indicating pre-adapted genotypes colonized different regions. Common gardens showed directional selection on flowering time that reversed between warm and cold sites, potentially maintaining clines. In the Great Basin, genomic predictions of strong local adaptation identified sites where cheatgrass is most dominant. Preventing new introductions that may fuel adaptation is critical for managing ongoing invasions.

Main Text: Biological invasions are a major cause of global change, but the mechanisms driving the most destructive invasions remain poorly understood(*1*). Is invasion success primarily determined by the susceptibility of invaded ecosystems(*2*), or are the worst invaders adapted to spread and dominate(*3*)? For example, local adaptation to the environment could increase fitness and abundance(*4*). On the other hand, colonizing genotypes may reach new environments to which they are maladapted, potentially hindering further spread(*5*,*6*). Furthermore, if the diversity of colonizing propagules is low, these new populations may be unable to adapt to new conditions(*7*), phenotypic plasticity of invasive genotypes may counteract local adaptation(*1*), or colonization bottlenecks may increase the frequency of deleterious mutations(*8*). Alternatively, if colonizing propagules are diverse, new populations may quickly adapt to local environments, facilitating invasive spread(*3*,*9*). Testing these hypotheses requires a rare combination of genomic, fitness, and abundance data(*10*).

Multiple mechanisms could contribute to local adaptation during invasions, generating distinct patterns of genomic and phenotypic variation(*11*,*12*). In general, selection may change along environmental gradients and promote clines of genotype and phenotype(*13*). If environmental gradients are similar in native versus invaded regions, clines may also be similar(*14*), consistent with niche conservatism between regions(*15*). Alternatively, if selective pressures are novel in the invaded range, clines may be unique, creating distinctive patterns of variation in native versus invaded regions(*16*–*18*). Furthermore, invasive genotypes may represent newly admixed populations(*19*), or form novel genotypes via introgression from congeners(*20*). Understanding extremely successful invasions thus requires dissecting global patterns of genomic and phenotypic variation, which has seldom been accomplished.

Bromus tectorum L. (cheatgrass) is a grass native to Eurasia and northern Africa that spread across North America by the 1890s(*21*, *22*), with devastating impacts in the arid and semi-arid ecosystems of the Intermountain West(*23*). It occurs in high abundance across an estimated 31% (210,000 km^2) of this region(*24*), displacing native perennials via rapid reproduction and shortened fire return intervals(*23*), reducing biodiversity and degrading wildlife habitat(*25*). It is a highly selfing, typically winter annual plant, with a high-quality reference genome (~2.5 Gb)(*22*,*26*). Existing genetic studies have been limited to small numbers of markers and populations, though they suggest that multiple introductions from different regions in Europe might have occurred in North America(*22*, *27*–*32*). Studies have shown evidence for local adaptation at small scales(*33*–*37*), but global patterns of local adaptation are unclear.

We aimed to identify the mechanisms and consequences of local adaptation in the North American cheatgrass invasion. We sequenced whole genomes of a global panel of 307 genotypes from the native and invaded ranges and measured phenotypes and performance in controlled experiments. We asked whether there were multiple and diverse introductions to North America and examined how geography and environment shape genomic diversity. We then evaluated if ancestry, trait, and allele frequency-environment clines were repeated in native and invasive genotypes, and if selection maintains clines. Finally, we assessed whether genomic matching to local climates facilitated invasive dominance.

Diverse native range ancestries invaded North America

Cheatgrass populations in North America stem from multiple, diverse introductions. Using ~267k unlinked single-nucleotide polymorphisms (SNPs), different clustering analyses of global genomic variation showed that population genetic structure largely followed geography in the

native range and to a lesser degree in North America (Fig. 1 showing K=4 genetic clusters, fig. S1). In the native range, west Asian, Mediterranean, and Atlantic genotypes primarily fell in a single cluster, while central and eastern European genotypes were mostly assigned to two clusters differentiated by latitude. In the invaded range, genotypes were assigned to all four clusters in western North America (WNA), but only to two clusters in eastern North America (ENA) (Fig. 1A–C, fig. S2). Most invasive genotypes were similar to genotypes from north-central-eastern Europe (Fig. 1D). In WNA, however, warm desert genotypes in southern California and Nevada were similar to genotypes in Iran and Afghanistan. The warm Mojave and the cool Pacific Northwest also harbored genotypes similar to those from the western Mediterranean (Fig. 1E,F). The diversity of genotypes found in WNA likely reflects colonization by propagules from different native regions.

High genome-wide diversity in WNA

Much of North America harbors great genomic diversity with little evidence of elevated genetic load (fig. S3,S4 using ~15.1M SNPs). In WNA, nucleotide diversity (π) was comparable to the most diverse native region, north-central-eastern Europe ($0.0016 \pm 4.5\times10^{-6}$ se vs. $0.0018 \pm 4.6\times10^{-6}$ se, respectively), followed by the Mediterranean ($0.0015 \pm 3.8\times10^{-6}$ se) and west Asia ($0.0011 \pm 3.1\times10^{-6}$ se), and was much lower in ENA ($0.0009 \pm 4.5\times10^{-6}$ se). In WNA, the skew in the site frequency spectrum (Tajima's D) was positively shifted (mean=2.8±0.006 se) indicating an excess of intermediate-frequency SNPs, consistent with strong population structure and variable ancestry across the region. In ENA, Tajima's D was low (mean=0.5±0.009 se) indicating more rare variants, suggesting recent population expansion. In the Mediterranean and north-central-eastern Europe, Tajima's D was positively shifted (Mediterranean mean=1.6±0.005, north-central-eastern Europe mean=2.2±0.007), suggesting substantial population substructure within these regions, while west Asian genotypes appeared more closely related to each other (Tajima's D mean=0.3±0.006).

To understand the effects of potential bottlenecks and drift in North America, we inspected variation in deleterious mutation load using ~15.1M SNPs (under the hypothesis that most protein changing mutations are deleterious). Estimated load was not different between native versus invaded range genotypes of the same ancestry (Tukey HSD on 2-way ANOVA p=0.3–1). The central-eastern European ancestry (dark green in fig. S4), widespread in North America, showed the lowest load in both ranges, suggesting large populations. In contrast, the west Asian and Mediterranean ancestry (pink in fig. S4) was associated with higher load in both ranges. Taken together, the high diversity in WNA indicates great potential for adaptation in this region.

Little isolation-by-distance but strong isolation-by-environment in North America

Both geography and environment shape genomic diversity in the native range, but geography plays a weak role in North America. Isolation-by-distance (based on ~267k SNPs) was strong in the native range (geographic vs. genetic distance Mantel $p=10^{-4}$, Fig. 2A) but very weak in North America (Mantel p=0.06, Fig. 2B). At 0–100 km distance we often found very unrelated genotypes in WNA (fig. S5A). Moreover, several groups in North America ("2–10" in Fig. 1E) composed of 4–14 near-clonal genotypes (>98% SNPs identity) were found across distances of >3000 km. In contrast, such far-flung, near-clonal genotypes were absent in the native range.

These patterns suggest long-distance dispersal (past or ongoing) within North America, introductions from distinct native range populations to nearby locations, and vice versa.

The weak spatial patterns in North America may reflect genotype sorting along the steep, heterogeneous climatic gradients that are common in WNA. Pairwise climatic distance (fig. S5B) significantly increased with spatial distance in both native and invaded ranges (Mantel $p=10^{-4}$ and Mantel correlation=0.6 in both ranges), but this relationship was weaker in WNA (Mantel correlation=0.3 WNA vs. 0.7 ENA; fig. S5C), reflecting the climatic heterogeneity of this region.

To examine genomic differentiation along climate gradients, we performed redundancy analysis (RDA) with variance partitioning, comparing the role of climate and spatial variables in explaining genomic variation. SNP variation was better explained by these predictors in the native than in the invaded range (native $R^2_{adj}=0.25$, invaded $R^2_{adj}=0.10$; Fig. 2C,D). Spatial variables explained little in North America (native $R^2_{adj}=0.07$, invaded $R^2_{adj}=0.005$), confirming low isolation-by-distance. In both ranges the abiotic environment explained the largest portion of SNP variation (native $R^2_{adj}=0.13$, invaded $R^2_{adj}=0.09$; Fig. 2E,F), highlighting the importance of isolation-by-environment in both the native and invaded range.

Repeated ancestry-climate clines in the native range and North America

Ancestry-environment clines were remarkably similar in the native and invaded ranges, suggesting environmental filtering of pre-adapted genotypes or directed gene flow (as opposed to local adaptation by novel genotypes). We focused on aridity and temperature gradients representative of global climatic variation in the cheatgrass range (see fig. S5B) and used generalized-additive-models (GAMs) to detect significant climate trends between ranges (fig. S6). In native and invasive genotypes, the west Asian and Mediterranean genetic cluster (pink) was more frequent in drier regions (GAM $p=0.0004$, pseudo-$R^2=0.5$), the northern Europe cluster (blue) was more frequent in humid regions (GAM $p=0.007$, pseudo-$R^2=0.08$), the central Europe cluster (dark green) was more frequent in regions with little precipitation seasonality (GAM $p=10^{-5}$, pseudo-$R^2=0.2$), and the northeast Europe ancestry (light green) was more frequent in regions with colder winters (GAM $p=0.002$, pseudo-$R^2=0.1$).

Repeated phenotype-climate clines in the native range and North America

Consistent with the hypothesis that pre-adaptation to local climate facilitated the cheatgrass invasion, we found similar phenotype-environment clines in the invaded and native ranges. To assess whether cheatgrass has phenotypic clines involved in local adaptation, we measured genetic variation among 169 native and invasive genotypes for eleven phenotypes in a growth chamber (data S1, table S1). A principal components (PC) analysis detected multi-trait axes of variation (Fig. 3A). PC1 explained 35.4% variation and suggests a life history axis of delayed flowering and high vegetative investment (more tillers and leaves) versus rapid flowering and high reproductive investment (taller, more fecund inflorescences). PC2 explained 22.2% variation and indicated an axis associated with larger plants with greater growth after vernalization versus shorter plants with little growth after vernalization. Native genotypes had on average earlier flowering and higher reproductive investment than invasive genotypes (t-test $p<0.01$ for PC1, flowering time, and individual seed mass) which may be due to different ancestry proportions in the native range. We found no significant native versus invasive trait

differences after accounting for relatedness, thus no evidence for evolution of increased competitive ability by invasive cheatgrass(*38*).

Multiple trait-climate clines potentially maintained by selection were mirrored between the native and invaded range (Fig. 3B). We focused on two climatic variables that we hypothesized would capture distinct climatic stressors: maximum vapor pressure deficit (Pa), which is a measure of aridity, and mean winter temperature (ºC) (fig. S5). To test for evidence of selection maintaining clines, we used linear-mixed models that accounted for genomic similarity (lmkin below), similar to Q_{ST}–F_{ST} tests(*39*). When significant, these models suggest selection is driving trait-climate clines, because the cline is stronger than expected by the genome-wide patterns of variation. In native and invasive genotypes, earlier flowering was associated with higher aridity (native lmkin-p=$2e^{-8}$, linear-R^2=0.5; invaded lmkin-p=0.03, linear-R^2=0.3), suggesting a locally adaptive cline of rapid phenology/early reproductive investment in arid regions versus delayed phenology/early vegetative investment in humid regions. Also, clines showed evidence of selection specifically within WNA, but not in ENA (fig. S7), consistent with the low genomic diversity of ENA. These patterns suggest genotypes pre-adapted to local climates now occur throughout WNA.

Selection on flowering time along a temperature gradient in WNA

Selection on flowering time changed direction between common gardens that differed in temperature. To test whether phenotypic clines in WNA were promoted by selection, we conducted two common garden experiments in different climates in Idaho with fall plantings across two years (2021 and 2022). One site was cooler (Sheep Station, ID, USA 44.2456ºN, 112.2144ºW, annual mean temperature 6ºC) and the other warmer (Wildcat, ID, USA 43.4744ºN, 116.9018ºW, annual mean temperature 12ºC). We planted 95 diverse genotypes from across WNA, for a total of 14,800 plants. We measured flowering time, survival, and fecundity.

In both years (Fig. 3C), selection favored later flowering at the cool site, with late flowering genotypes often having 3× the fitness of earlier flowering genotypes (~300 vs. ~100 seeds produced per original sown seed). By contrast, at the warm site, selection favored earlier flowering, with the earliest flowering genotypes often having >10× the fitness of the later flowering genotypes (*e.g.*, ~170 vs. ~17 seeds produced per original sown seed). This suggests that late flowering genotypes have an extreme disadvantage in warm climates. This strong selection is consistent with our finding that the hottest sites in WNA were almost exclusively comprised of west Asian-like genotypes. We saw no clear admixture from distantly related, but geographically proximate European-like genotypes inhabiting cooler and wetter higher elevations (Fig. 1A), suggesting a barrier to maladapted immigrants. Thus, the climate gradients in WNA appear to impose changes in selection maintaining a strong phenotypic cline.

Repeated allele frequency-climate clines in the native range and WNA

Putative quantitative trait loci (QTL) for traits under selection showed similar allele frequency-climate clines in the invaded and native ranges (Fig. 4, fig. S8–S9). Using genome-wide association studies (GWAS), we identified several genetic loci associated with trait variation (data S2). We highlight flowering time QTL with annotations based on homology to known genes in other species(*26*).

The top flowering time QTL contained multiple SNPs along a haploblock of ~28 Mb (chromosome 1: 56–84 Mb, allele frequency (AF)~0.9) containing 64 genes with annotations based on homology to *Oryza sativa* and *Arabidopsis thaliana*. These genes were enriched for Gene Ontology terms describing developmental processes involving reproductive structure/system, embryo, embryo ending in seed dormancy, post-embryonic, fruit, and seed (8 *O. sativa* genes and 14 *A. thaliana* genes, $p<0.0003$, FDR=0.01). Such a large haploblock could indicate a structural variant, a potential driver of local adaptation(*40*, *41*); this locus merits further investigation.

The top SNP of the haploblock (chromosome 1: 71007448 bp, AF=0.91) was 25 kb downstream of a *O. sativa* homolog, the DnaJ protein ERDJ3B. Expression of ERDJ3B is critical for heat stress tolerance during seed development(*42*). Late flowering alleles were more frequent in humid/colder regions of the native range and WNA (Fig. 4A–C), suggesting cheatgrass adaptation to cold might be linked to seed sensitivity to temperature stress.

The fourth top flowering time QTL comprised three SNPs (chromosome 1: 236616590 bp, 236616999 bp, 236617691 bp, AF=0.82) 0.5 kb upstream (putative promoter region) of the *A. thaliana* homolog ATE1 (AT5G05700). ATE1 regulates seed maturation, seedling metabolism, and abscisic acid (ABA) germination sensitivity(*43*). Early flowering alleles were associated with lineages from drier regions, corresponding to the closely related native Mediterranean-west Asia, and invaded Mojave-Lahontan Basin, but also reaching Mediterranean climates of coastal WNA (Fig. 4D–F). These patterns suggest that even the specific mutations underlying local adaptation are operating in the invaded range.

Stronger predicted local adaptation where cheatgrass dominates

Whole genome-environment associations in the native range predicted local adaptation in the invaded range, especially where cheatgrass is most dominant. To further evaluate whether invasive genotypes matched local climates as in the native range, we used a predictive genome-environment model. Using the native range RDA model of genotype based on climate (Fig. 2E), we predicted invasive genotypes for locations of our sequenced samples, and calculated the genetic distance between predicted and observed genotypes, similar to the 'genomic offset'(*44*). Genotype-environment matching (*i.e.*, low genetic distance, or offset, between predicted and observed genotypes) was strongest at northern latitudes across North America, particularly in WNA. Putative maladaptation (*i.e.*, high genetic distance between predicted and observed genotypes) was strongest in the southeast USA (Fig. 5A). By comparing mean genetic distance to means of 1000 null permutations, we found the mean genetic distance was significantly lower than the null in WNA ($p<0.002$), but not in ENA ($p=0.5$, Fig. 5B). This finding is consistent with the hypothesis that local adaptation to climate in WNA has repeated the patterns of the native range and may facilitate invasion, while cheatgrass in ENA has a different strategy. Unlike WNA, cheatgrass populations in ENA are more restricted to an ephemeral life history in highly disturbed urban and agricultural sites, rarely forming large monospecific stands(*45*).

To assess whether matching of specific genotypes to local environments promotes cheatgrass invasion, we compared the strength of genotype-environment correlations with variation in cheatgrass abundance from 11,307 field surveys across the Great Basin (Fig. 5A, polygon), where the invasion has its worst impacts(*24*). Locations where cheatgrass occurs in high abundance showed high genotype-environment matching based on the native range model (N=55, t-test $p=0.006$, Fig. 5C), suggesting local adaptation promotes cheatgrass dominance.

This pattern was consistent when comparing genotype-environment matching of high-abundance sites to 1,000 null permutations of genotypes within the Great Basin (p=0.01), evidence that this pattern was not merely due to environmental characteristics of the low-abundance sites but reflects the match of genotypes to their local environments.

Synthesis

Biological invasions pose a major environmental threat, but the role of genomic diversity and adaptation is poorly understood. Our results have general implications for understanding the role of adaptation in the success of devastating invasions. Multiple diverse introductions and long-distance dispersal post-introduction likely increased the chances of cheatgrass genotypes finding suitable environments. In turn, local adaptation via environmental filtering of pre-adapted genotypes contributed to the success of invasive populations. Local adaptation could also be due to selection on newly admixed populations(*19*) but we found no novel admixed genotypes in the invaded compared to the native range. Instead, our results suggest that climate gradients can drive coordinated physiology-life cycle strategies shared across ranges, consistent with niche conservatism in North America(*15,46*).

In WNA, selection regimes associated with temperature likely maintain a major life history cline, with the most locally adapted populations being the most ecologically dominant. Dominance could facilitate further dispersal and colonization creating more opportunities to reach matched climates. Our common garden results also indicate that genetic diversity (*e.g.*, for flowering time) is critical to maintaining fitness across a temperature gradient. Our findings emphasize that ongoing introductions can contribute to adaptation in already established, naturalized, invasive species(*47*). Limiting incoming diversity could likely minimize the cheatgrass potential for rapid adaptation under climate change.

References

1. E. Z. Daly, O. Chabrerie, F. Massol, B. Facon, M. C. M. Hess, A. Tasiemski, F. Grandjean, M. Chauvat, F. Viard, E. Forey, L. Folcher, E. Buisson, T. Boivin, S. Baltora-Rosset, R. Ulmer, P. Gibert, G. Thiébaut, J. H. Pantel, T. Heger, D. M. Richardson, D. Renault, A synthesis of biological invasion hypotheses associated with the introduction–naturalization–invasion continuum. *Oikos* **2023**, e09645 (2023).

2. D. Liu, F. Essl, B. Lenzner, D. Moser, P. Semenchuk, T. M. Blackburn, P. Cassey, D. Biancolini, C. Capinha, W. Dawson, E. E. Dyer, B. Guénard, E. Economo, H. Kreft, J. Pergl, P. Pyšek, M. van Kleunen, C. Rondinini, H. Seebens, P. Weigelt, M. Winter, A. Purvis, S. Dullinger, Regional invasion history and land use shape the prevalence of non-native species in local assemblages. *Glob. Chang. Biol.* **30**, e17426 (2024).

3. R. I. Colautti, S. C. H. Barrett, Rapid adaptation to climate facilitates range expansion of an invasive plant. *Science* **342**, 364–366 (2013).

4. M. C. Urban, S. Y. Strauss, F. Pelletier, E. P. Palkovacs, M. A. Leibold, A. P. Hendry, L. De Meester, S. M. Carlson, A. L. Angert, S. T. Giery, Evolutionary origins for ecological patterns in space. *Proc. Natl. Acad. Sci.* **117**, 17482–17490 (2020).

5. M. Kirkpatrick, N. H. Barton, Evolution of a species' range. *Am. Nat.* **150**, 1–23 (1997).

6. E. Mayr, *Animal Species and Evolution* (Harvard University Press, 1963; https://doi.org/10.4159/harvard.9780674865327).

7. C. G. Eckert, K. E. Samis, S. C. Lougheed, Genetic variation across species' geographical ranges: the central–marginal hypothesis and beyond. *Mol. Ecol.* **17**, 1170–1188 (2008).

8. J. Robinson, C. C. Kyriazis, S. C. Yuan, K. E. Lohmueller, Deleterious variation in natural populations and implications for conservation genetics. *Annu Rev Anim Biosci*. **11**, 93–114 (2023).

9. V. I. Simón-Porcar, J. L. Silva, M. Vallejo-Marín, Rapid local adaptation in both sexual and asexual invasive populations of monkeyflowers (*Mimulus* spp.). *Ann. Bot.* **127**, 655–668 (2021).

10. R. A. Bay, R. J. Harrigan, V. L. Underwood, H. L. Gibbs, T. B. Smith, K. Ruegg, Genomic signals of selection predict climate-driven population declines in a migratory bird. *Science* **359**, 83–86 (2018).

11. A. Nota, S. Bertolino, F. Tiralongo, A. Santovito, Adaptation to bioinvasions: When does it occur? *Glob. Chang. Biol.* **30**, e17362 (2024).

12. C. Rosche, I. Hensen, A. Schaar, U. Zehra, M. Jasieniuk, R. M. Callaway, D. P. Khasa, M. M. Al-Gharaibeh, Y. Lekberg, D. U. Nagy, R. W. Pal, M. Okada, K. Schrieber, K. G. Turner, S. Lachmuth, A. Erst, T. Tsunoda, M. Sheng, R. Schmidt, Y. Peng, W. Luo, Y. Jäschke, Z. A. Reshi, M. A. Shah, Climate outweighs native vs. nonnative range-effects for genetics and common garden performance of a cosmopolitan weed. *Ecol. Monogr.* **89**, e01386 (2019).

13. J. S. Santangelo, et al., Global urban environmental change drives adaptation in white clover. *Science* **375**,1275–1281 (2022).

14. E. A. Leger, K. J. Rice, Assessing the speed and predictability of local adaptation in invasive California poppies (*Eschscholzia californica*). *J. Evol. Biol.* **20**, 1090–1103 (2007).

15. C. Liu, C. Wolter, W. Xian, J. M. Jeschke, Most invasive species largely conserve their climatic niche. *Proc. Natl. Acad. Sci.* **117**, 23643–23651 (2020).

16. K. G. Turner, K. L. Ostevik, C. J. Grassa, L. H. Rieseberg, Genomic analyses of phenotypic differences between native and invasive populations of diffuse knapweed (*Centaurea diffusa*). *Front. Ecol. Evol.* **8**, 577635 (2021).

17. J. M. Kreiner, A. Caballero, S. I. Wright, J. R. Stinchcombe, Selective ancestral sorting and de novo evolution in the agricultural invasion of *Amaranthus tuberculatus*. *Evolution* **76**, 70–85 (2022).

18. S. B. Endriss, C. Alba, A. P. Norton, P. Pyšek, R. A. Hufbauer, Breakdown of a geographic cline explains high performance of introduced populations of a weedy invader. *J. Ecol.* **106**, 699–713 (2018).

19. M. Vallejo-Marín, J. Friedman, A. D. Twyford, O. Lepais, S. M. Ickert-Bond, M. A. Streisfeld, L. Yant, M. Van Kleunen, M. C. Rotter, J. R. Puzey, Population genomic and historical analysis suggests a global invasion by bridgehead processes in *Mimulus guttatus*. *Commun. Biol.* **4**, 327 (2021).

20. V. C. Bieker, P. Battlay, B. Petersen, X. Sun, J. Wilson, J. C. Brealey, F. Bretagnolle, K. Nurkowski, C. Lee, F. S. Barreiro, G. L. Owens, J. Y. Lee, F. L. Kellner, L. Van Boheemen, S. Gopalakrishnan, M. Gaudeul, H. Mueller-Schaerer, S. Lommen, G. Karrer, B. Chauvel, Y. Sun, B. Kostantinovic, L. Dalén, P. Poczai, L. H. Rieseberg, M. T. P. Gilbert, K. A. Hodgins, M. D. Martin, Uncovering the genomic basis of an extraordinary plant invasion. *Sci. Adv.* **8**, eabo5115 (2022).

21. R. N. Mack, Invasion of *Bromus tectorum* L. into western North America: An ecological chronicle. *Agro-Ecosyst.* **7**, 145–165 (1981).

22. S. J. Novak, R. N. Mack, "Chapter 4. Mating system, introduction and genetic diversity of *Bromus tectorum* in North America, the most notorious product of evolution within *Bromus* section Genea" in *Exotic Brome-Grasses in Arid and Semiarid Ecosystems of the Western US: Causes, Consequences, and Management Implications*, M. J. Germino, J. C. Chambers, C. S. Brown, Eds. (Springer International Publishing, 2016), pp. 99–132.

23. M. J. Germino, J. Belnap, J. M. Stark, E. B. Allen, B. M. Rau, "Chapter 3. Ecosystem impacts of exotic annual invaders in the genus *Bromus*" in *Exotic Brome-Grasses in Arid and Semiarid Ecosystems of the Western US: Causes, Consequences, and Management Implications*, M. J. Germino, J. C. Chambers, C. S. Brown, Eds. (Springer International Publishing, 2016), pp. 61–95.

24. B. A. Bradley, C. A. Curtis, E. J. Fusco, J. T. Abatzoglou, J. K. Balch, S. Dadashi, M.-N. Tuanmu, Cheatgrass (*Bromus tectorum*) distribution in the intermountain western United States and its relationship to fire frequency, seasonality, and ignitions. *Biol. Invasions* **20**, 1493–1506 (2018).

25. L. M. Porensky, D. M. Blumenthal, Historical wildfires do not promote cheatgrass invasion in a western Great Plains steppe. *Biol. Invasions* **18**, 3333–3349 (2016).

26. S. R. Revolinski, P. J. Maughan, C. E. Coleman, I. C. Burke, Preadapted to adapt: Underpinnings of adaptive plasticity revealed by the downy brome genome. *Commun. Biol.* **6**, 326 (2023).

27. S. J. Novak, R. N. Mack, P. S. Soltis, Genetic variation in *Bromus tectorum* (Poaceae): Introduction dynamics in North America. *Can. J. Bot.* **71**, 1441–1448 (1993).

28. S. J. Novak, R. N. Mack, Tracing plant introduction and spread: Genetic evidence from *Bromus tectorum* (Cheatgrass). *BioScience* **51**, 114 (2001).

29. M. T. Valliant, R. N. Mack, S. J. Novak, Introduction history and population genetics of the invasive grass *Bromus tectorum* (Poaceae) in Canada. *Am. J. Bot.* **94**, 1156–1169 (2007).

30. L. J. Schachner, R. N. Mack, S. J. Novak, *Bromus tectorum* (Poaceae) in midcontinental United States: Population genetic analysis of an ongoing invasion. *Am. J. Bot.* **95**, 1584–1595 (2008).

31. T. D. Huttanus, R. N. Mack, S. J. Novak, Propagule pressure and introduction pathways of *Bromus tectorum* (cheatgrass; Poaceae) in the central United States. *Int. J. Plant Sci.* **172**, 783–794 (2011).

32. A. R. Pawlak, R. N. Mack, J. W. Busch, S. J. Novak, Invasion of *Bromus tectorum* (L.) into California and the American southwest: Rapid, multi-directional and genetically diverse. *Biol. Invasions* **17**, 287–306 (2015).

33. E. A. Leger, E. K. Espeland, K. R. Merrill, S. E. Meyer, Genetic variation and local adaptation at a cheatgrass (*Bromus tectorum*) invasion edge in western Nevada. *Mol. Ecol.* **18**, 4366–4379 (2009).

34. R. A. Hufft, T. J. Zelikova, "Chapter 5. Ecological Genetics, Local Adaptation, and Phenotypic Plasticity in Bromus tectorum in the Context of a Changing Climate" in *Exotic Brome-Grasses in Arid and Semiarid Ecosystems of the Western US: Causes, Consequences, and Management Implications*, M. J. Germino, J. C. Chambers, C. S. Brown, Eds. (Springer International Publishing, Cham, Switzerland, 2016) *Springer Series on Environmental Management*, pp. 133–154.

35. S. E. Meyer, P. S. Allen, Ecological genetics of seed germination regulation in *Bromus tectorum* L. II. Reaction norms in response to a water stress gradient imposed during seed maturation. *Oecologia* **120**, 35–43 (1999).

36. S. E. Meyer, P. S. Allen, Ecological genetics of seed germination regulation in *Bromus tectorum* L. I. Phenotypic variance among and within populations. *Oecologia* **120**, 27–34 (1999).

37. S. E. Meyer, D. L. Nelson, S. L. Carlson, Ecological genetics of vernalization response in *Bromus tectorum* L. (Poaceae). *Ann. Bot.* **93**, 653–663 (2004).

38. J. L. Hierro, Ö. Eren, J. Čuda, L. A. Meyerson, Evolution of increased competitive ability may explain dominance of introduced species in ruderal communities, *Ecol. Monogr.* **92**, e1524 (2022).

39. J. K. McKay, R. G. Latta, Adaptive population divergence: Markers, QTL and traits. *Trends Ecol. Evol.* **17**, 285–291 (2002).

40. M. Todesco, G. L. Owens, N. Bercovich, J.-S. Légaré, S. Soudi, D. O. Burge, K. Huang, K. L. Ostevik, E. B. Drummond, I. Imerovski, Massive haplotypes underlie ecotypic differentiation in sunflowers. *Nature* **584**, 602–607 (2020).

41. P. Battlay, J. Wilson, V. C. Bieker, C. Lee, D. Prapas, B. Petersen, S. Craig, L. Van Boheemen, R. Scalone, N. P. De Silva, A. Sharma, B. Konstantinović, K. A. Nurkowski, L. H. Rieseberg, T. Connallon, M. D. Martin, K. A. Hodgins, Large haploblocks underlie rapid adaptation in the invasive weed *Ambrosia artemisiifolia*. *Nat. Commun.* **14**, 1717 (2023).

42. F. Resentini, G. Orozco-Arroyo, M. Cucinotta, M. A. Mendes, The impact of heat stress in plant reproduction. *Front. Plant Sci.* **14**, 1271644 (2023).

43. T. J. Holman, P. D. Jones, L. Russell, A. Medhurst, S. Úbeda Tomás, P. Talloji, J. Marquez, H. Schmuths, S.-A. Tung, I. Taylor, S. Footitt, A. Bachmair, F. L. Theodoulou, M. J. Holdsworth, The N-end rule pathway promotes seed germination and establishment through removal of ABA sensitivity in *Arabidopsis*. *Proc. Natl. Acad. Sci.* **106**, 4549–4554 (2009).

44. C. Gain, B. Rhoné, P. Cubry, I. Salazar, F. Forbes, Y. Vigouroux, F. Jay, O. François, A quantitative theory for genomic offset statistics. *Mol. Biol. Evol.* **40**, msad140 (2023).

45. L. A. Morrow, P. W. Stahlman, The history and distribution of Downy Brome (*Bromus tectorum*) in North America. *Weed Sci.* **32**, 2–6 (1984).

46. A. NA, M. U. Shaanker, P. Bhat HN, B. Charles, U. Shaanker R, M. A. Shah, Niche shift in invasive species: is it a case of "home away from home" or finding a "new home"? *Biodivers. Conserv.* **31**, 2625–2638 (2022).

47. A. L. Smith, T. R. Hodkinson, J. Villellas, J. A. Catford, A. M. Csergő, S. P. Blomberg, E. E. Crone, J. Ehrlén, M. B. Garcia, A.-L. Laine, D. A. Roach, R. Salguero-Gómez, G. M. Wardle, D. Z. Childs, B. D. Elderd, A. Finn, S. Munné-Bosch, M. E. A. Baudraz, J. Bódis, F. Q. Brearley, A. Bucharova, C. M. Caruso, R. P. Duncan, J. M. Dwyer, B. Gooden, R. Groenteman, L. N. Hamre, A. Helm, R. Kelly, L. Laanisto, M. Lonati, J. L. Moore, M. Morales, S. L. Olsen, M. Pärtel, W. K. Petry, S. Ramula, P. U. Rasmussen, S. R. Enri, A. Roeder, C. Roscher, M. Saastamoinen, A. J. M. Tack, J. P. Töpper, G. E. Vose, E. M. Wandrag, A. Wingler, Y. M. Buckley, Global gene flow releases invasive plants from environmental constraints on genetic diversity. *Proc. Natl. Acad. Sci.* **117**, 4218–4227 (2020).

48. Dryad dataset for this study with repository DOI will be available here.

49. S. Andrews, FastQC: A quality control tool for high throughput sequence data [Online], version 0.11.8 (2010); http://www.bioinformatics.babraham.ac.uk/projects/fastqc/.

50. A. M. Bolger, M. Lohse, B. Usadel, Trimmomatic: a flexible trimmer for Illumina sequence data. *Bioinformatics* **30**, 2114–2120 (2014).

51. B. Bushnell, BBTools package, version 38.90 (2014); https://sourceforge.net/projects/bbmap/.

52. H. Li, R. Durbin, Fast and accurate short read alignment with Burrows–Wheeler transform. *bioinformatics* **25**, 1754–1760 (2009).

53. H. Li, B. Handsaker, A. Wysoker, T. Fennell, J. Ruan, N. Homer, G. Marth, G. Abecasis, R. Durbin, The sequence alignment/map format and SAMtools. *Bioinformatics* **25**, 2078–2079 (2009).

54. T. S. Korneliussen, A. Albrechtsen, R. Nielsen, ANGSD: Analysis of next generation sequencing data. *BMC Bioinformatics* **15**, 1–13 (2014).

55. P. Danecek, J. K. Bonfield, J. Liddle, J. Marshall, V. Ohan, M. O. Pollard, A. Whitwham, T. Keane, S. A. McCarthy, R. M. Davies, Twelve years of SAMtools and BCFtools. *Gigascience* **10**, giab008 (2021).

56. S. R. Browning, B. L. Browning, Rapid and accurate haplotype phasing and missing-data inference for whole-genome association studies by use of localized haplotype clustering. *Am. J. Hum. Genet.* **81**, 1084–1097 (2007).

57. B. L. Browning, Y. Zhou, S. R. Browning, A one-penny imputed genome from next-generation reference panels. *Am. J. Hum. Genet.* **103**, 338–348 (2018).

58. R Core Team, R: A Language and Environment for Statistical Computing, R Foundation for Statistical Computing (2021); https://www.R-project.org/.

59. X. Zheng, D. Levine, J. Shen, S. M. Gogarten, C. Laurie, B. S. Weir, A high-performance computing toolset for relatedness and principal component analysis of SNP data. *Bioinformatics* **28**, 3326–3328 (2012).

60. S. Purcell, B. Neale, K. Todd-Brown, L. Thomas, M. A. Ferreira, D. Bender, J. Maller, P. Sklar, P. I. De Bakker, M. J. Daly, PLINK: A tool set for whole-genome association and population-based linkage analyses. *Am. J. Hum. Genet.* **81**, 559–575 (2007).

61. P. M. Bourke, R. E. Voorrips, C. A. Hackett, G. van Geest, J. H. Willemsen, P. Arens, M. J. Smulders, R. G. Visser, C. Maliepaard, Detecting quantitative trait loci and exploring chromosomal pairing in autopolyploids using polyqtlR. *Bioinformatics* **37**, 3822–3829 (2021).

62. D. N. Karger, O. Conrad, J. Böhner, T. Kawohl, H. Kreft, R. W. Soria-Auza, N. E. Zimmermann, H. P. Linder, M. Kessler, Climatologies at high resolution for the earth's land surface areas. *Sci. Data* **4**, 1–20 (2017).

63. D. N. Karger, O. Conrad, J. Böhner, T. Kawohl, H. Kreft, R. W. Soria-Auza, N. E. Zimmermann, H. P. Linder, M. Kessler, Climatologies at high resolution for the earth's land surface areas, EnviDat (2021); https://doi.org/10.16904/envidat.228.

64. J. Hollister, T. Shah, elevatr: Access elevation data from various APIs, version 0.99.0 (2017); http://github.com/usepa/elevatr.

65. R. S. Bivand, E. J. Pebesma, V. Gómez-Rubio, E. J. Pebesma, *Applied Spatial Data Analysis with R* (Springer, 2008) vol. 747248717.

66. R. J. Hijmans, raster: Geographic data analysis and modeling, version 3.6-26 (2023); https://rspatial.org/raster.

67. Commission for Environmental Cooperation Working Group, *Ecological Regions of North America – toward a Common Perspective* (Commission for Environmental Cooperation, Montreal, Canada, 1997).

68. J. Oksanen, G. Simpson, F. Blanchet, R. Kindt, P. Legendre, P. Minchin, R. O'Hara, P. Solymos, M. Stevens, E. Szoecs, H. Wagner, M. Barbour, M. Bedward, B. Bolker, D. Borcard, G. Carvalho, M. Chirico, M. De Caceres, S. Durand, H. B. A. Evangelista, R. FitzJohn, M. Friendly, B. Furneaux, G. Hannigan, M. O. Hill, L. Lahti, D. McGlinn, M.-H. Ouelette, E. R. Cunha, T. Smith, A. Stier, C. J. F. Ter Braak, J. Weedon, vegan: Community ecology package, version 2.6-4 (2022); https://CRAN.R-project.org/package=vegan.

69. L. Skotte, T. S. Korneliussen, A. Albrechtsen, Estimating individual admixture proportions from next generation sequencing data. *Genetics* **195**, 693–702 (2013).

70. J. Meisner, A. Albrechtsen, Inferring population structure and admixture proportions in low-depth NGS data. *Genetics* **210**, 719–731 (2018).

71. G. Evanno, S. Regnaut, J. Goudet, Detecting the number of clusters of individuals using the software STRUCTURE: a simulation study. *Mol. Ecol.* **14**, 2611–2620 (2005).

72. H. Wickham, W. Chang, M. H. Wickham, Package 'ggplot2.' *Create Elegant Data Vis. Using Gramm. Graph. Version* **2**, 1–189 (2016).

73. N. Saitou, M. Nei, The neighbor-joining method: A new method for reconstructing phylogenetic trees. *Mol. Biol. Evol.* **4**, 406–425 (1987).

74. W.-C. Chen, "Overlapping codon model, phylogenetic clustering, and alternative partial expectation conditional maximization algorithm," thesis, Iowa State University (2011).

75. E. Paradis, K. Schliep, ape 5.0: an environment for modern phylogenetics and evolutionary analyses in R. *Bioinformatics* **35**, 526–528 (2019).

76. M. Nei, Analysis of gene diversity in subdivided populations. *Proc. Natl. Acad. Sci.* **70**, 3321–3323 (1973).

77. B. S. Weir, J. Goudet, A unified characterization of population structure and relatedness. *Genetics* **206**, 2085–2103 (2017).

78. J. Goudet, Hierfstat, a package for R to compute and test hierarchical F-statistics. *Mol. Ecol. Notes* **5**, 184–186 (2005).

79. M. Nei, W.-H. Li, Mathematical model for studying genetic variation in terms of restriction endonucleases. *Proc. Natl. Acad. Sci.* **76**, 5269–5273 (1979).

80. P. Danecek, A. Auton, G. Abecasis, C. A. Albers, E. Banks, M. A. DePristo, R. E. Handsaker, G. Lunter, G. T. Marth, S. T. Sherry, The variant call format and VCFtools. *Bioinformatics* **27**, 2156–2158 (2011).

81. F. Tajima, Statistical method for testing the neutral mutation hypothesis by DNA polymorphism. *Genetics* **123**, 585–595 (1989).

82. P. Cingolani, A. Platts, L. L. Wang, M. Coon, T. Nguyen, L. Wang, S. J. Land, X. Lu, D. M. Ruden, A program for annotating and predicting the effects of single nucleotide polymorphisms, SnpEff. *Fly (Austin)* **6**, 80–92 (2012).

83. G. Pertea, M. Pertea, GFF utilities: GffRead and GffCompare. *F1000Res.* **9**, PMC7222033 (2020).

84. J. A. F. Diniz-Filho, T. N. Soares, J. S. Lima, R. Dobrovolski, V. L. Landeiro, M. P. de C. Telles, T. F. Rangel, L. M. Bini, Mantel test in population genetics. *Genet. Mol. Biol.* **36**, 475–485 (2013).

85. S. Dray, A.-B. Dufour, The ade4 package: Implementing the duality diagram for ecologists. *J. Stat. Softw.* **22**, 1–20 (2007).

86. R. M. Gutaker, S. C. Groen, E. S. Bellis, J. Y. Choi, I. S. Pires, R. K. Bocinsky, E. R. Slayton, O. Wilkins, C. C. Castillo, S. Negrão, M. M. Oliveira, D. Q. Fuller, J. A. d'Alpoim Guedes, J. R. Lasky, M. D. Purugganan, Genomic history and ecology of the geographic spread of rice. *Nat. Plants* **6**, 492–502 (2020).

87. T. Capblancq, B. R. Forester, Redundancy analysis: A Swiss army knife for landscape genomics. *Methods Ecol. Evol.* **12**, 2298–2309 (2021).

88. S. Dray, P. Legendre, P. R. Peres-Neto, Spatial modelling: A comprehensive framework for principal coordinate analysis of neighbour matrices (PCNM). *Ecol. Model.* **196**, 483–493 (2006).

89. S. Dray, D. Bauman, G. Blanchet, D. Borcard, S. Clappe, G. G. T. Jombart, G. Larocque, H. H. Wagner, adespatial: Multivariate Multiscale Spatial Analysis, version 0.3-23 (2018); https://github.com/sdray/adespatial.

90. D. Bauman, T. Drouet, M.-J. Fortin, S. Dray, Optimizing the choice of a spatial weighting matrix in eigenvector-based methods. *Ecology* **99**, 2159–2166 (2018).

91. S. N. Wood, Fast stable restricted maximum likelihood and marginal likelihood estimation of semiparametric generalized linear models. *J. R. Stat. Soc. Ser. B Stat. Methodol.* **73**, 3–36 (2011).

92. E. B. Josephs, J. J. Berg, J. Ross-Ibarra, G. Coop, Detecting adaptive differentiation in structured populations with genomic data and common gardens. *Genetics* **211**, 989–1004 (2019).

93. T. M. Therneau, coxme: Mixed effects cox models, version 2.2-20 (2022); https://CRAN.R-project.org/package=coxme.

94. X. Zhou, M. Stephens, Genome-wide efficient mixed-model analysis for association studies. *Nat. Genet.* **44**, 821–824 (2012).

95. F. Tian, D.-C. Yang, Y.-Q. Meng, J. Jin, G. Gao, PlantRegMap: Charting functional regulatory maps in plants. *Nucleic Acids Res.* **2019**, gkz1020 (2019).

Acknowledgments: Any opinions, findings, conclusions, or recommendations expressed in the material are those of the authors and should not be construed to represent any official USDA determination or policy. This product (article, paper, etc.) has been peer reviewed and approved for publication consistent with USGS Fundamental Science Practices (https://pubs.usgs.gov/circ/1367/). Any use of trade, firm, or product names is for descriptive purposes only and does not imply endorsement by the U.S. Government. Xavier Mack, Carlos Rodríguez-Gonzalez, Yuxin Luo, and Katherine Blocklove helped with measuring phenotypes, harvesting, and performing DNA extractions. Ian Burke, Samuel Revolinski, Peter Maughan, and Craig Coleman granted us access to the reference genome prior to publication. iNaturalist was a key resource for identifying seed collectors, among those were also Dave Barnett, David Board, Chalon Boesel, John Bradford, Jaime Braschi, Howard Bruner, Victoria Bustamante, Charles Campbell, Jeanne Chambers, Mike Chen, Mark Chynoweth, Jason Cooper, Massimo Cristofaro, Melodie Cunningham, Kirk Davies, Janelle Downs, Torsten Eriksson, Maggie Eshleman, Erica Fleishman, Carol Kadonsky & Bill Foreman, Berit Gehrke, Tom Getts, Richard Gill, Dana Hartel, Nate Hartley, Patricia Hollins, Alex Hood, Tayla Hook, Parker Hopkins, Becky Hufft, Jennifer Kalt, Lorri Kendrick, Molly Ladd, Matt Lavin, Steven Lee, Jonathan Levine, Marisa Mancillas, John Maron, Grace McCartha, Randal Mindell, Chandra Moffat, Brooke Moore, James Nagler, Yael Orgad, Matthew Pedrotti, David Pyke, Sasha Reed, Matt Rinella, Viktoria Ropak, Håkan Rydin, Geno Schupp, Adam Searcy, Tim Springer, Amy Symstad, Tracy Thomas, Trudy Trevarthen, Samantha vanDeurs, Biljana Vidovic, Viktoria Wagner, Gretchen Whetham, David Wilderman, Eileen Wyza, and Pauline & Jon Zweck. In loving memory of Bill Foreman.

Funding:

National Science Foundation grant DEB-1927282 (PBA), DEB-1927009 (JRL), DEB-1927177 (MBH).

Joint Genome Institute of the U.S. Department of Energy Office of Science grant New Investigator Award-506608 (JRL).

National Institutes of Health grant R35GM138300 (JRL).

Author contributions:

Conceptualization: DG, CSB, EAL, DMB, MJG, LMP, MBH, PBA, JRL

Methodology: DG, TMM, NP, SR, AP, CSB, EAL, DMB, MJG, LMP, MBH, PBA, JRL

Investigation: DG, MLV, AD, RB-Z, EAL, DMB, MJG, LMP, PBA, JRL, OB, CSB, RB, SB-M, SMC, SLD-F, AD, RCD, PWD, DJE, TAV, HH, MCH, RAH, SJ, JMK, EK, SK,

MK, AK, ML, SL, DM, CLM, JWM, DUN, JPO, RP, LAP, LR, BGR, CR, MS, RKS, AS, BMS, RLS, KGT, AKU, AVW, C-AW, JZ.

Funding acquisition: PBA, MBH, JRL, MJG

Project administration: PBA, MBH, CSB, DMB, MJG, LMP, JRL

Writing – original draft: DG, JRL

Writing – review & editing: all authors

Competing interests: Authors declare that they have no competing interests.

Data and materials availability: Seeds of *Bromus tectorum* genotypes used in this study are available from the lead contact upon request. Whole-genome sequences (.bam files) are being deposited in the European Nucleotide Archive (ENA; https://www.ebi.ac.uk/ena). Whole-genome sequences (.fastq files) for four genotypes sequenced by the DOE Joint Genome Institute are publicly available at their website under proposal ID: 506608. The .beagle (genotype-likelihoods), .vcf (SNP calls), raw phenotype data, and common garden flowering time and fitness data are publicly available at Dryad, with DOI available upon publication(*48*). Genotype coordinates, climate data, and phenotypes are in Data S1.

List of Supplementary Materials:

Materials and Methods

Figs. S1 to S9

Table S1

References (*49*–*95*)

Data S1 to S2

Fig. 1: The cheatgrass invasion involved multiple diverse introductions from the native range to North America (**A**) Admixture proportions for K=4 ancestral genetic clusters (colors) for invasive and native genotypes in different regions; WNA: western North America (n=107), ENA: eastern North America (n=67), out: not in North America (n=8), MD: Mediterranean (n=24), NCE EU: north-central-east Europe (n=53), WA: west Asia (n=28). Geographic distribution of (**B**) invasive (n=194, North American only) and (**C**) native (n=105) genotypes. (**D**) Genetic differentiation (F_{ST}) between native and invaded regions, with notations following panel A. (**E**) Principal components analysis showing PC1 (y-axis) and PC2 (x-axis) explaining 20.6% of genomic variation. Axes are shifted to better reflect the latitudinal distribution of genotypes. Gray letters denote geographic origin in the native range. Black numbers mark groups of invasive genotypes: 1 warm desert genotypes, 2–10 quasi-clonal genotypes found up to 3000 km apart (2 includes one from Germany). (**F**) Neighbor-joining tree annotated with native (gray letters) and invaded locations (black numbers and starts). Native notations follow the ISO alpha-3 country code or their cardinal direction in Europe (EU). Numbers are as in panel E. Stars mark branches with invasive genotypes.

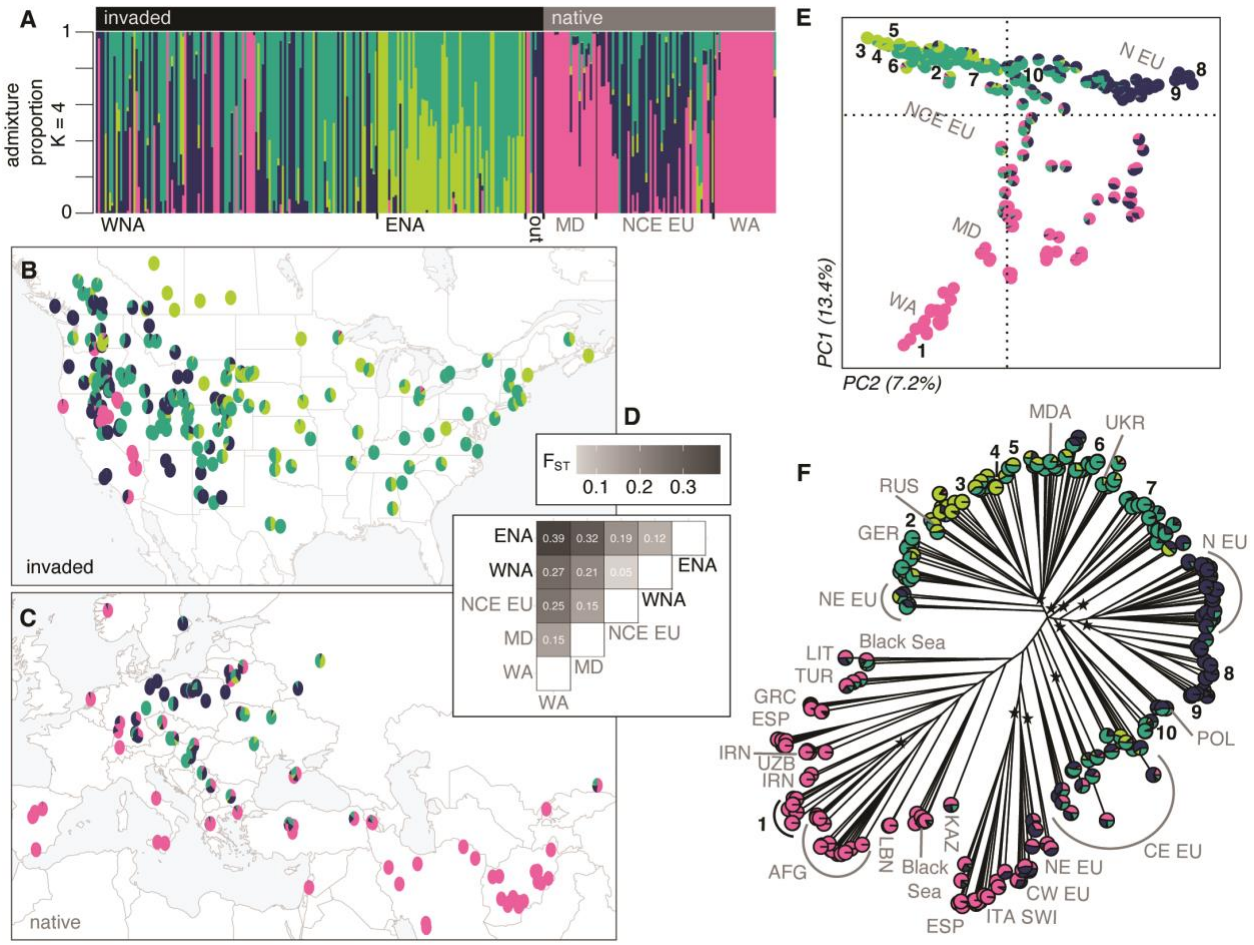

Fig. 2: Genomic variation is structured by environment in the native and invaded ranges. Strong isolation-by-distance in the (**A**) native but not in the (**B**) invaded range (**Mantel p=10^{-4}); plots show raw pair-wise data with a spline. Euler Plots show genomic variation is best explained by both the abiotic environment and spatial distance in (**C**) the native range, but only by the abiotic environment in (**D**) the invaded range. Fields of squares represent total genomic variation, circles represent genomic variation explained by a particular group of variables calculated using variance partitioning with RDA ordination (native n=105, invaded n=194). (**E**) Native and (**F**) invasive genotypes projected on the first two canonical axes of RDA (x-axis: RDA1 y-axis: RDA2). Arrows represent environmental predictors that strongly correlate with a maximal proportion of variation in linear combinations of SNPs. ELV: elevation, PET: potential evapotranspiration, PRC: total annual precipitation, PSE: precipitation seasonality, TAR: temperature annual range, TDR: temperature diurnal range, TMP: annual mean temperature. Colors are K=4 ancestral clusters. Geographic annotations are depicted in bolded black; N EU: north Europe, E EU: east Europe, C EU: central Europe, MD: Mediterranean, WA: west Asia, W coast: west coast, InterM. W: intermountain west, ENA: eastern North America.

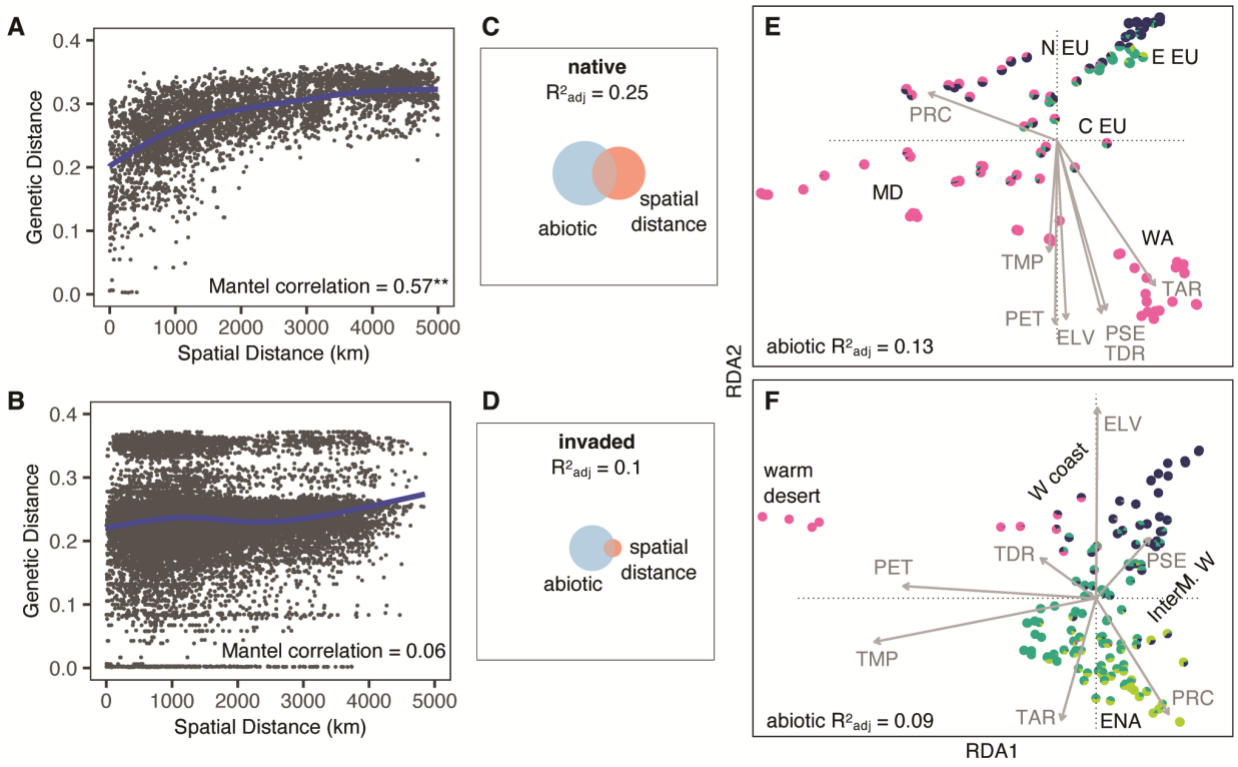

Fig. 3: Selection along aridity and temperature gradients shapes flowering phenology. (**A**) Eigenvector plot with loadings of eleven phenotypes onto PC1 (x-axis) and PC2 (y-axis) describing axes of life history variation of 169 genotypes in a growth chamber; fl: Flowering, n: Number, inflor: Inflorescence. (**B**) Growth chamber phenotype-environment associations for invasive (left; n=138–145) and native genotypes (right; n=31–36). Coefficients of determination (R^2), trends (gray lines), and 95% confidence intervals (gray shades) come from linear regressions. Significance comes from linear-mixed kinship models that accounted for relatedness among genotypes: *p<0.05, ***p<0.0001. (**C**) Fitness advantage of early flowering genotypes at a warm site/common garden (WI: Wild Cat, gray crosses) and of late flowering genotypes at a cool site/common garden (SS: Sheep Station, gray open circles) in two consecutive years (top: 2022 harvest and bottom: 2023 harvest). Trends (gray lines) and 95% confidence intervals (gray shades) come from linear regressions. Significance comes from linear-mixed kinship models of fitness (seed count for 2022 and inflorescence mass for 2023) in response to mean first day of flowering (fl), site, and their interaction (int): *p<0.05, **p<0.005, ***p<0.0005. In all panels colors are K=4 ancestral clusters.

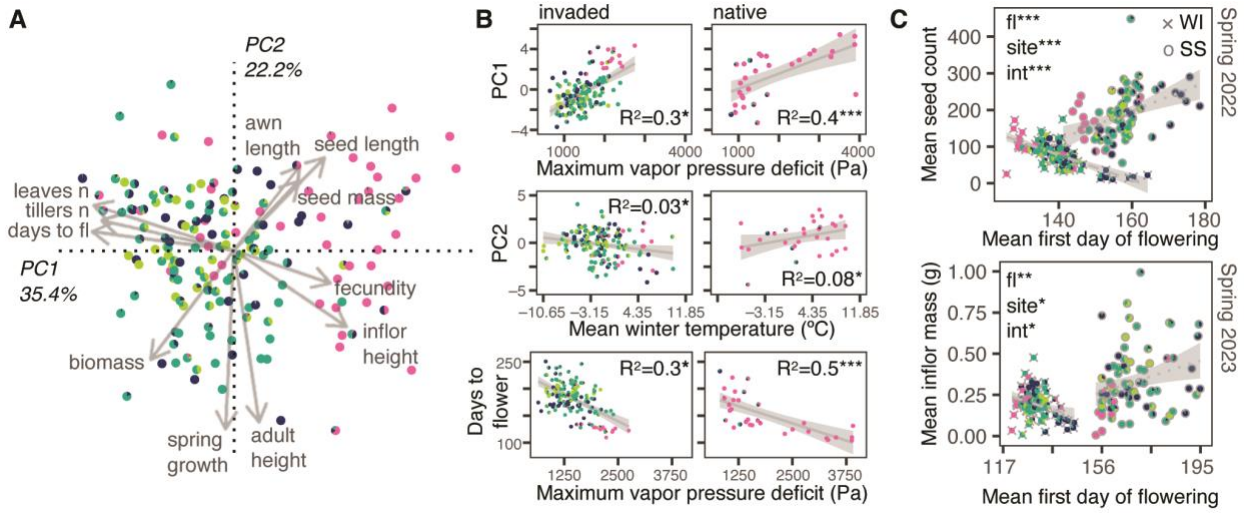

Fig. 4: Environmental trends of two flowering time QTL are mirrored between native and invasive genotypes. (**A** and **D**) Geographic distribution of QTL SNP alleles in the native (top) and invaded (bottom) range; crosses represent the reference/major (ref) allele, and open circles the alternate/minor (alt) allele. (**B** and **E**) Zoomed-in Manhattan plots showing Wald-test *p*-values (plotted as $-\log_{10}$) from GWAS and genomic location of top SNP (marked in green), with respective false-discovery-rate (FDR) and minor allele frequency (MAF). (**C** and **F**) Phenotypic (boxplots to the left) and environmental variation (boxplots to the right) of flowering time QTL SNP alleles (alt and ref) identified with GWAS. ***p<0.0008 from a two-sampled t-test, but no significant differences were detected from linear-mixed effects models that accounted for genetic similarity among genotypes. Max VPD: Maximum vapor pressure deficit in kPa.

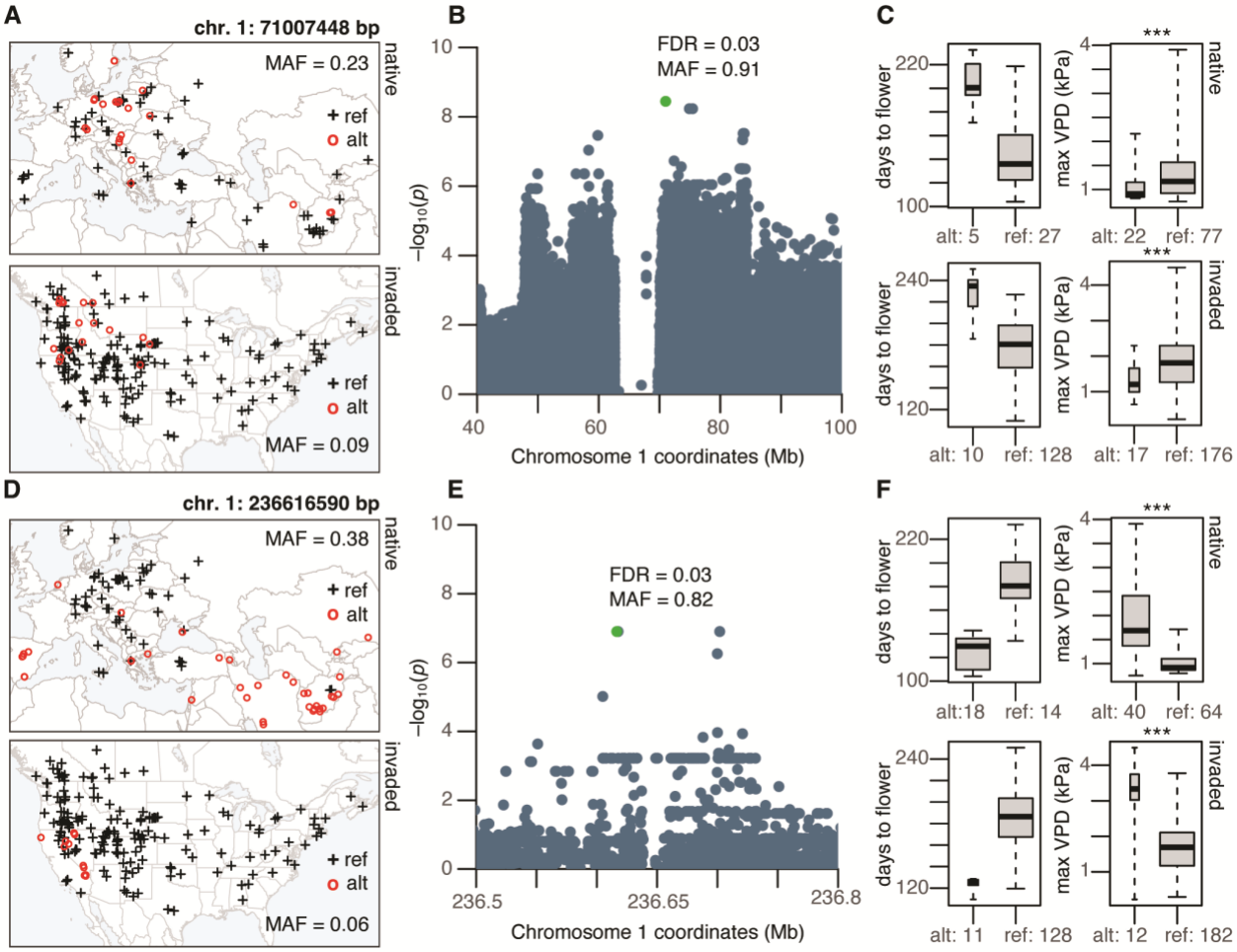

Fig. 5: Genomic predictions of strong local adaptation occur in regions where cheatgrass is most dominant. (**A**) Geographic distribution of the genomic offset estimated for each invasive genotype. The genomic offset or maladaptation is the genetic distance between observed invasive genotypes and the genotype-environment predictions in the invaded range based on the native range genotype-environment association. (**B**) Histograms of the mean genetic distance (offset) of 1000 null permutations in western North America (WNA) and eastern North America (ENA), relative to their estimated mean genetic distance (red lines). (**C**) Within the Great Basin (polygon in **A**), the mean genetic distance (offset) is significantly lower in areas where cheatgrass occurs in high (*i.e.*, representing >15% vegetation cover) vs. low abundance.